Communication in Physical Sciences, 2021, 7(4): 312-320

Latitudinal ionospheric Responses to Full Halo CMEs Induced Geomagnetic Storm

Dominic Chukwuebuka Obiegbuna*, Francisca Nneka Okeke, Kingsley Chukwudi Okpala, Sivla William Tafon and Orji Prince Orji

Received: 11 November 2021/Accepted 04 December 2021/Published online: 15 December 2021

Abstract: *We have studied and compared the effects of full halo CMEs induced geomagnetic storms across the high, mid/equatorial and low latitude ionosphere around Ny Alesund, Norway, Irkutsk, Russia and Adis Ababa, Ethiopia. The total electron content (TEC) data obtained from the global positioning system (GPS) were used to examine the level of responses of ionospheric latitudes to full halo CMEs induced geomagnetic storms of June 23rd 2015. This study was carried out using dual frequency ground based GNSS observations at high latitude (NYAL: 78.56°N, 11.52°E), mid-latitude (IRKM: 52.13°N, 106.24°E) and low (Adis: 9.02°N, 38.44°E), ionospheric stations. The vertical TEC (VTEC) was extracted from Receiver Independent Exchange (RINEX) formatted GPS-TEC data using the GOPI Software developed by Seemala Gopi. The GOPI software is a GNSS-TEC analysis program that uses ephemeris data and differential code biases (DCBs) in estimating slant TEC (STEC) before its conversion to VTEC. The result showed positive ionospheric responses of the ionospheric latitudes on the storm day. The overall responses across the latitudes to the geomagnetic storm were generally positive for the high latitude and negative for mid/equatorial and low latitudes.*

Keywords: *Geomagnetic storm, Full Halo CMEs, High Latitude, Low latitude, Ionosphere, TEC*

Dominic Chukwuebuka Obiegbuna,
[1]Department of Science Laboratory Technology, University of Nigeria, Nsukka, Nigeria
[2] Department of Physics and Astronomy, University of Nigeria, Nsukka, Nigeria
Email: dominic.obiegbuna@unn.edu.ng
Orcid id: 0000-0002-8339-0272

Francisca Nneka Okeke
Department of Physics and Astronomy, University of Nigeria, Nsukka, Enugu State, Nigeria
Email: fracisca.okeke@unn.edu.ng
Orcid id: 0000-0002-4662-3145

Kingsley Chukwudi Okpala
Department of Physics and Astronomy, University of Nigeria, Nsukka, Enugu State, Nigeria
Email: kingsley.okpala@unn.edu.ng
Orcid id: 0000-0002-4662-3145

Sivla William Tafon
Department of Physics and Astronomy, University of Nigeria, Nsukka, Enugu State, Nigeria
Email: william.sivla@unn.edu.ng
Orcid id: 0000-0003-0281-5505

Orji Prince Orji
Department of Physics and Astronomy, University of Nigeria, Nsukka, Enugu State, Nigeria
Email: : prince.orji@unn.edu.ng
Orcid id: 0000-0003-2825-7046

1.0 Introduction

Storm causing solar winds otherwise known as geoeffective solar winds (Gonzalez *et al*.,

1994) is characterized by prolonged and enhanced southward biased interplanetary magnetic fields (B_s) that allow for efficient transportation of particles and energies from solar wind streams into the earth's magnetosphere. Geoeffective solar wind streams associated with geomagnetic storms have been shown to result from coronal mass ejections (CMEs) (Cane *et al*., 2000; Webb *et al*., 2000). Corona mass ejections are classified based on their appearances on the occulting disc of the observing coronagraph. They are halo and non-halo CMEs. Non-halo CMEs are not visible on the coronagraphs, while halo CMEs which are visible on the occulting disc of the coronagraph are either full ($W = 360^o$) or partial ($120^o \leq W < 360^o$) depending on the apparent width of CMEs (Gopalswamy, 2009). Usually, halo CMEs are high-speed, wide and are associated mostly with flares of very high X-ray since only very energetic CMEs spread out rapidly to become visible on the occulting disks early in the event (Gopalswamy *et al*., 2008).

A geomagnetic storm is a consequence of chains of events that are initiated at the sun. Particles and energy depositions into the Earth's magnetosphere by solar winds lead to the formation of ring current which in turn causes diamagnetism. This diamagnetism creates a disturbance in the Earth's magnetic field. These disturbances are observed as variations in the horizontal component of the earth's magnetic field (Echer *et al*., 2008). These disturbances of the earth's magnetic fields are called geomagnetic storms. The major mechanism employed in the explanation of geomagnetic storms as a consequence of the solar wind- magnetosphere coupling process is the principle of magnetic reconnection. The magnetic reconnection entails the interconnection of the oppositely inclined interplanetary magnetic field (IMF) and geomagnetic field. This coupling of the solar wind and the magnetosphere eventually results in the exchange of plasma, energy and momentum between the various magnetic field regions (Hughes, 1995). The efficiency of this reconnection process is determined by the geoeffectiveness of the solar wind (Dungey, 1961; Perreault and Akasofu, 1978; Tsuruntani and Gonzalez, 1997).

The consequential outcome of the solar wind - magnetosphere – ionosphere coupling is the changes observed in the ion production and loss rates which eventually lead to spatial and temporal variations in ionospheric parameters like total electron content (TEC) (Rishbeth, 1998). Another consequence of the solar wind – magnetosphere – ionosphere coupling is the development of ring currents around the earth's equator which induces perturbations in the H component of the earth's magnetic field also known as geomagnetic storm. Geomagnetic storms are either recurrent or non recurrent depending on their nature of occurrences. The parameter used in measuring the magnitude of geomagnetic disturbances is the disturbance storm time (Dst) index and it is proportional to the kinetic energy of particles present in the outer radiation belt (Gonzalez *et al*., 1994).

Most often, the main driver of ionospheric dynamics in the high latitude region is coupling between the solar wind, magnetosphere and ionosphere (Watson, 2016). Hence, the high latitude ionosphere is controlled by particles and electric fields from the magnetosphere (Hunsucker and Hargreaves, 2003). These particles are deposited into the high latitude ionosphere from the magnetosphere by particle precipitations and joule heating (Sharma *et al*., 2020). When particles, energy and momentum precipitate into the higher latitudes from the thermosphere, energy is transmitted to the neutral gas from the aurora electric current via joule heating. The neural winds move down to the lower latitudes by momentum transfer. Equator bound gravity waves are produced by the joule heating and momentum transfer of the thermospheric winds and pressure (Nava *et al*., 2016).

These electric fields and neutral winds enter the mid and subsequently low latitudes, while the equatorial plasma flows into the region along magnetic field lines. This causes plasma instabilities which affect the plasma content by varying the ionospheric plasma altitude in so doing determine the rate of recombination. Except for the equator bound neutral winds caused by the Joule heating of the high latitude thermosphere, the Disturbance Dynamo Electric field (DDEF) (Yeh *et al*., 1991; Abdu *et al*., 2012 and Devi *et al*., 2018) and direct Prompt Penetrations of dawn-dusk Electric Field (PPEF) also penetrate the equatorial and low latitude ionosphere eventually leading to storm time modification of the currents and fields of that region (Sastri *et al*., 1997; Monti *et al*., 2015). These lead to changes in plasma densities and dynamics. The PPEF is generated by neutral winds. They are eastward in day times and westward at nighttime (Heelis, 2004; Fuller-Rowell, 2011). PPEF develops promptly and enhances the dynamo-electric field, which also initiates the vertical $E \times B$ plasma drift at the magnetic dip equator, thus lifting the plasma to higher altitudes. This effect is known as the fountain effect and is usually stronger on the dayside and post-sunset period at the low and equatorial latitude regions. Contrary to the PPEF, the DDEF builds up slowly and takes several hours to set up the disturbance winds associated with it, after which they can persist for hours (Maruyama *et al*., 2005; Astafyeva *et al*., 2017).

Using the total electron content (TEC) data, this study examined the responses of the low latitude (Adis: 9.02^{o}N, 38.44^{o}E), mid-latitude (IRKM: 52.13^{o}N, 106.24^{o}E) and high latitude (Nyal: 78.56^{o}N, 11.52^{o}E) ionospheres to full halo CMEs induced geomagnetic storm of June 23rd, 2015 and also to investigate the level of impact of the storm to the ionospheres.

2.0 Materials and Methods

This study has been carried out using the dual frequency ground based GNSS observations at high (NYAL: 78.56^{o}N, 11.52^{o}E), mid (IRKM: 52.13^{o}N, 106.24^{o}E) and low (ADIS: 9.02^{o}N, 38.44^{o}E) latitude ionospheric stations in Ny Alesund, Russia, Svalbard, Norway and Adis Ababa, Ethiopia. The raw TEC data was obtained in a RINEX format. The GPS-TEC program software developed by Seemala Gopi was used to calculate and extract the vertical TEC (VTEC) using the differential carrier phase and pseudo range observations (Seemala and Valladares, 2011). The GNSS-TEC analysis program uses ephemeris data and differential code biases (DCBs) for calculating and approximating slant TEC (STEC). The noises in the pseud orange TEC data are removed by using the carrier phase labeling method to smoothen the GNSS pseud orange. Equation (1) was used in calculating the STEC along with the satellite receiver.

$$STEC = VTEC + B \quad (1)$$

The B in equation (1) is the instrument bias. In other words, by removing the instrument biases, STEC is converted to VTEC. The STEC is converted to VTEC using equation (2) below:

$$VTEC = STEC \times (1 - (\frac{R_E \cos(\alpha)}{R_E + h_{max}}))^{1/2} \quad (2)$$

R_E is the radius of the earth, α is the elevation cut off and h_{max} is the of ionospheric pierce point (IPP) altitude. The elevation cut-off is usually assumed to be greater than 20^o to avoid the errors resulting from tropospheric effects, multipath and changes in the geometry of satellites. While the ionospheric pierce point (IPP) is usually considered to be 350 Km.

TEC variation generally denoted as ΔTEC (change in the TEC) is calculated using equation (3):

$$\Delta TEC = TEC_s - TEC_q \quad (3)$$

where TEC_s is the storm time TEC and TEC_q is the average of the 5 quietest days of the month (reference ionosphere). They will be denoted herein as disturbed day TEC (Dd TEC) and quiet day TEC (Sq TEC). The quiet (reference ionosphere) was obtained by using the five international quietest days of each month of interest (Okpala *et al*., 2020). The months used

in this study are June and December 2015 and January 2016. The ith hour averages of those 5 days are obtained using equation (3):

$$TEC_q = \frac{1}{5}\sum_{j=1}^{5} C_{ij} \quad (4)$$

where C_{ij} represents the raw VTEC for a particular hour (i = 1 to 24) for a given quietest day (j = 1 to 5).

The percentage VTEC has been calculated to show the level of changes in VTEC values during storm days. It is obtained using equation (5):

$$\%TEC = \frac{(TEC_s - TEC_{q)}}{TEC_s} \times 100 \quad (5)$$

TEC_s and TEC_q have been defined above.

The disturbance storm (Dst) index which is a measure of magnetic activities were obtained from the World Data Center, Kyoto, Japan (http://wdc.kugi.kyoto-u.ac.jp/dst_provisional/index.html).

There are three categories of Dst data therein: the real time, Provisional and the final indices. The WDC provided the final Dst from 1957 to 2014 and the provisional Dst from 2015 to 2016 as at the time of this study. The ACE satellite provided the B_z component of the interplanetary magnetic field (IMF), the solar wind speed V_{sw} and proton density .These are key parameters for storm studies (https://omniweb.gsfc.nasa.gov/). The dawn-dusk component of the interplanetary electric field (IEF) E_y, is computed using equation (6) as given by Zhao *et al*., 2008.

$$E_y = -B_z \times V_{sw} \times 10^{-3} \quad (6)$$

Where E_y the interplanetary electric field (IEF) is measured in (mV/m), B_z in (nT) and V_{sw} is in (Km/s).

3.0 Results and Discussions

We have investigated the response of high, mid and low latitude ionospheres over NYAL (78.56°N, 11.52°E), IRKM (52.13°N, 106.24°E) and ADIS (9.02°N, 38.44°E) in Ny Alesund, Russia, Svalbard, Norway and Adis Ababa, Ethiopia to full and partial halo geomagnetic storm of 23rd June 2015.

3.1 Geomagnetic storm event of 23rd June 2015

The diurnal variation of the interplanetary magnetic field, IMF-Bz, interplanetary electric field IEF (E_y), and disturbance storm time (Dst) which are background geophysical, solar and interplanetary conditions have been used to study the storm of 23rd June 2015. They are as shown in Figure 1 below. The storm has been defined as a full halo geomagnetic storm (Wantari, 2017).

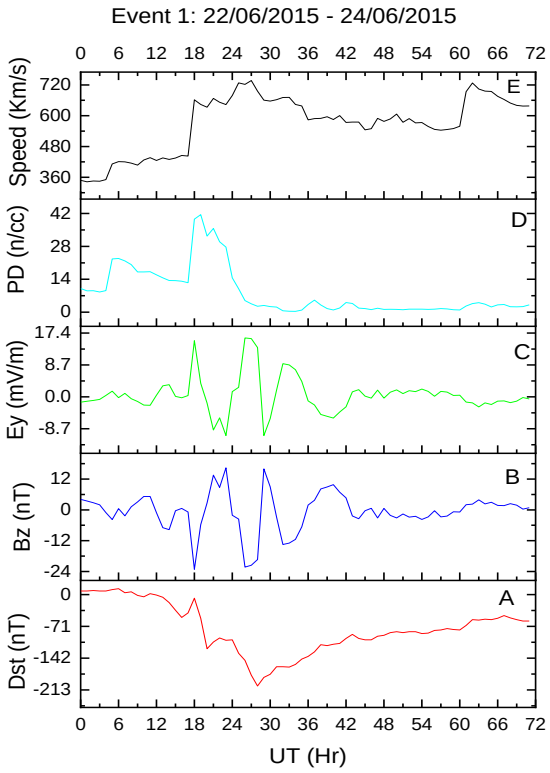

Fig. 1: (a) Disturbance storm index (Dst) (b) Interplanetary magnetic field (Bz) (c) Interplanetary electric field (Ey) (d) Proton density (e) Solar wind speed for the geomagnetic storm event

The Geomagnetic storm event started from 22nd June to 24th June 2015. From Figure 1 (a), it is seen that the storm had a sudden commencement. It started from 00:00 UT with a Dst value of 8 nT and got to its minimum Dst value of -204 nT at about 04:00 UT on 23rd before making a gradual and consistent recovery to its quiet time value. It took more

than 24 hours for the Dst to recover to its pre-storm level. The Dst signature showed multiple steps variations before its peak which is substorms of magnitudes 50nT and 113 nT. They lasted for four hours between 12:00 UT and 16:00 UT and two hours between 18:00 UT and 20:00 UT respectively. The plot of the variation of the interplanetary magnetic (Bz) and electric field (Ey) are shown alongside the Dst variation in Figure 1(b and c). There was an excellent but negative correlation between the IMF-Bz and IEF (Ey). In other words, when IMF-Bz is southward, IEF (Ey) is eastward and vis-a-viz. The storms and sub-storms have been shown to have occurred when the interplanetary electric field IEF (Ey) is eastward (i.e positive) and IMF Bz is southward (negative). The interplanetary electric field is observed to peak between one and two hours before the occurrences of the sub storms and storms. For instance, while IEF (Ey) peaked at 15:00 UT, 19:00 UT and 02:00 UT, the geomagnetic substorms and storms occurred at times 16:00 UT, 20:00 UT and 04:00 UT respectively. On the contrary, the interplanetary magnetic field (Bz) decreases to its minimum values an hour or two before the occurrence of storms.

It is also seen from the proton density plot in Figure 1(d), that the sub storms and storms correspond with an enhanced particle influx (proton density peak). The proton density got to its maximum value of 41.48 n/cc at 20:00 UT an hour before the substorm and 9 hours before the main storm. It is pertinent to note, that the proton densities intensified when the IMF Bz remained southward and also coincided with sub storms formation. These substorms processes contribute an immense amount of energy to the ring current intensification which also is a key factor in the occurrences of geomagnetic storms (Sandhu *et al*., 2018). The time between the proton density peaks and geomagnetic substorms occurrences indicates the time between the influx of energetic particles into the magnetosphere responsible for energy intensification and formation of ring current which in turn causes disturbances in the magnetic field of the earth.

3.2 Ionospheric response to the storm

A plot of VTEC variations across low (ADIS), mid (IRKM) and high (NYAL) latitude ionosphere during a geomagnetic storm event of 23rd June 2015 are shown in Figure 2. The VTEC which represents TEC showed unique signatures at the various latitudes. The disturbed TEC showed a positive response to the storm at ADIS only on the storm day. The disturbed TEC was higher than quiet mean VTEC by 5.59 TECU at 06:00UT (09:00 LT), 4.82 TECU at 12:00UT (15:00 LT) and 5.61 TECU at 22:00 UT (01:00 LT on 23rd), these differences accounted for about 13.54%, 10.50%, and 51.92% variations respectively. However, before the storm peak day, there was a sharp decrease in TEC from 22.51 TECU at 17:00UT (20:00 LT) to 2.53 TECU at 22:00UT (01:00 LT on 23rd). Meanwhile at the mid-latitude IRKM, disturbed TEC started showing an increment of up to 57.89% for quiet mean TEC on 22nd starting from 01:00 UT (9:00 LT) to 18:00 UT (02:00 LT on 23rd). Double positive responses of magnitudes 7.26 TECU and 6.39 TECU were observed at 28:00 UT (12:00 LT) and 37:00 UT (21:00 LT) respectively on 23rd June. The disturbed TEC was higher than the mean quiet TEC by 6.42 TECU and 6.03 TECU at the above mentioned times respectively.

There was also about 67.23% decrement in disturbed VTEC from the mean quiet TEC observed at 48:00 UT (10:00 LT) on the 24th of June. On the other hand, NYAL showed very visible enhancements before the storm day. However, at the time of maximum mean quiet TEC at 07:00 UT (09:00 LT) on 22nd June, there was a depletion of disturbed TEC. There was an enhancement in VTEC on 06:00 UT (07:00 LT) and a depletion an hour later, before an enhancement from 08:00 UT (09:00 LT). A day after the storm, depletion in VTEC was observed between 00:00 UT (01:00 LT) and

07:00 UT (08:00 LT) before enhancements for the rest of the day.

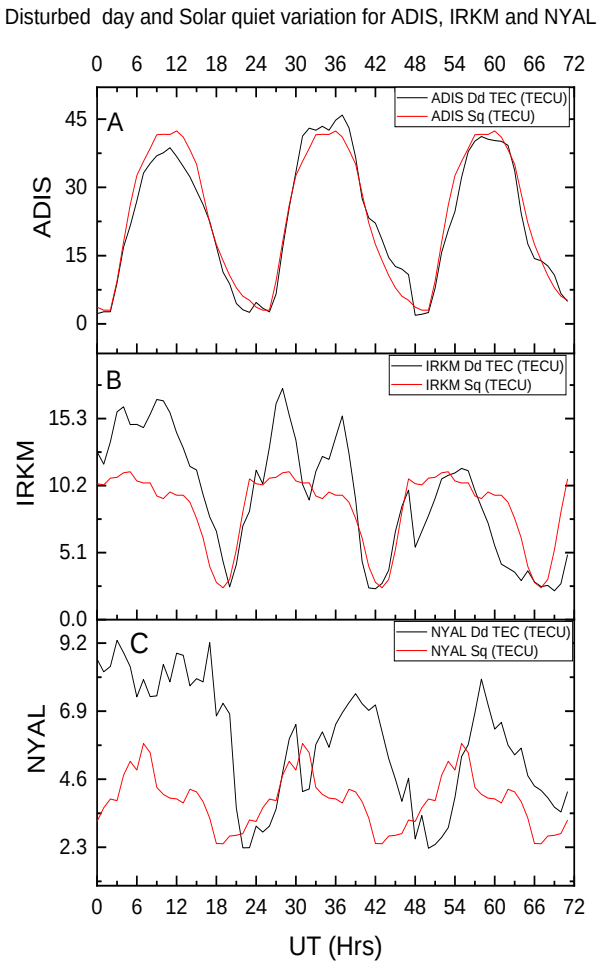

Fig. 2: Disturbed TEC (Dd TEC) and Solar quiet (Sq) plots for (a) ADIS (b) IRKM and (c) NYAL

Percentage variation has been used to understand the extent of the impact of a geomagnetic storm on TEC across the latitudes before the storm, storm day and post-storm day. A plot of percentage variation of TEC was plotted as shown in Figure 3. Unlike ADIS and IRKM, NYAL showed an unusual response to the storm. The enhancement of disturbed TEC began long before the storm started.

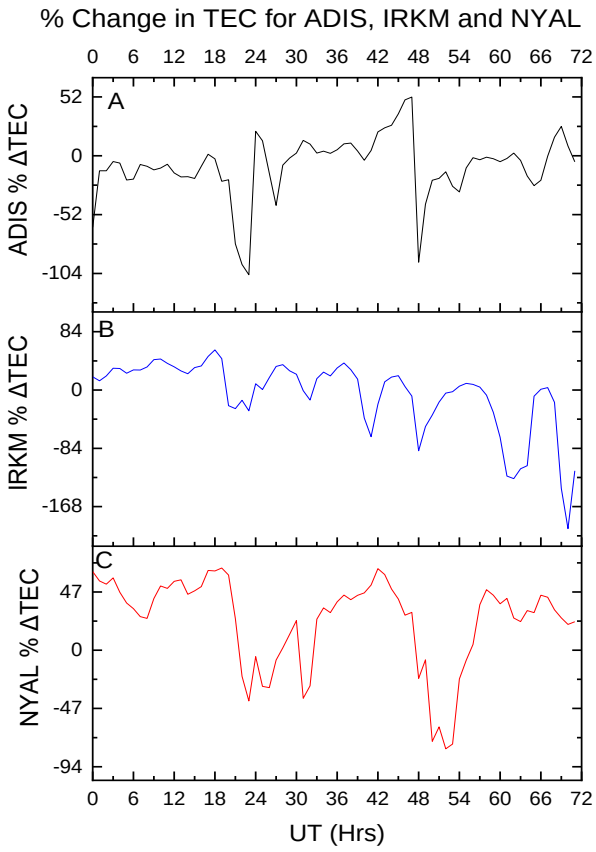

Fig. 3: Percentage change in TEC for (a) ADIS (b) IRKM (c) NYAL

The percentage variation of TEC was observed to be 63.93% a day before the storm peak which is on 22nd of June. On the storm day which is the 23rd of June, the disturbed TEC was higher than the mean quiet VTEC with 4.68 TECU which is about 65.82% variation. NYAL experienced a post storm enhancement in TEC which was up to 48.82%, unlike the low and mid latitude stations. While ADIS and NYAL showed positive responses, IRKM showed a negative response of diurnal variation of TEC on June 23rd, 2015. However, ADIS and IRKM showed overall negative responses, while NYAL responded positively to the geomagnetic storm event.

From the results above, possible effects of particle precipitations into the magnetosphere-ionosphere system is seen in the early hours of the storm event. The high rate of particle and energy depositions in the course of

geomagnetic storm events occasioned the heating and expansion of the thermosphere. This led to the creation of a pressure gradient and a consequent global thermospheric circulation (Forbes, 1989; Buosuanto *et al*., 1999). The thermospheric circulations cause variations in the O/N_2 ratio which leads to fluctuations in production/ loss rates of ions and therefore the positive/negative ionospheric storm otherwise known as increment/decrement in TEC observed at the high latitudes.

However, at the mid/ equatorial and low latitudes, the nature and magnitudes of these ionospheric storms are dependent on the peculiar electrodynamics of the latitudes. For example, the Prompt penetration electric field which is major electrodynamics in the mid and low latitudes is one of the determinants of ionospheric behaviors. The PPEFs when westwards (dusk to dawn) on the night side causes a downward drift or negative ionospheric storm and when eastwards (dawn to dusk) on the daysides causes significant ionospheric uplift and positive ionospheric storms (Astafyeva *et al*., 2018).

4.0 Conclusion

The responses of the high, mid and low latitude ionosphere to full halo CMEs induced geomagnetic storms have been studied. The full halo CMEs induced geomagnetic storm which peaked on the 23rd of June, 2015 with magnitude -215 nT, started on 22nd and recovered on the 24th June. The overall responses of the low and mid-latitude stations to the geomagnetic storm event were negative, which that of the high latitude was positive. However, all the latitudes showed positive responses to the storm on the storm peak day. ADIS a low latitude station showed negative responses a day before and after the storm peak day. Mid-latitude IRKM only showed a negative response on the storm recovery day while high latitude NYAL responded positively throughout.

5.0 Acknowledgement

We sincerely wish to acknowledge the World Data Center, Kyoto, Japan, the National Aeronautics and Space Administration for allowing us to access their data bases and finally to Professor Seemala Gopi for making his GPS-TEC Analysis software accessible.

6.0 References

Abdu, M. A., Batista, I. S., Bertoni, F., Reinisch, B.W., Kherani, E. A. & Sobral, J. H. A. (2012), Equatorial ionosphere responses to two magnetic storms of moderate intensity from conjugate point observations in Brazil. *Journal of Geophysical Research*, 117, A05321. Doi: 10.1029/2011JA017174

Astafyeva, E., Zakharenkova, I., Hozumi, K., Alken, P., Coïsson, P., Hairston, M. R., & Coley, W. R., (2018), Study of the equatorial and low-latitude electrodynamic and ionospheric disturbances during the 22–23 June 2015 geomagnetic storm using ground-based and space borne techniques. *Journal of Geophysical Research: Space Physics*, 123. doi.org/10.1002/2017JA024981

Devi, M., S. Patgiri, A. K. Barbara, G. Gordiyenko, A., Depueva, V. & Ruzhin, Y. Y. (2018), Storm Time Ionospheric-Tropospheric Dynamics: a Study Through Ionospheric and Lower Atmospheric Variability Features of High/Mid and Low Latitudes. *Geomagnetism and Aeronomy*. 58, 7, pp. 857–870. Doi.: 10.1134/S001679321807 006X

Dungey, J. W. (1961). Interplanetary Magnetic Field and the Auroral Zones. *Physical Review Letters*, 6, 2, 47–48. doi:10.1103/physrevlett.6.47

Echer, E., Gonzalez, W.D., Tsurutani, B. T. & Gonzalez, A. L. C. (2008), Interplanetary conditions leading to superintense geomagnetic storms (Dst < _250) during solar cycle 23. *Geophysical Research Letter*, 35, L06S03, doi:10.1029/2007GL031755.

Fuller-Rowell, T. J. (2011), Storm-Time Response of the Thermosphere–Ionosphere System. *Aeronomy of the Earth's Atmosphere and Ionosphere*, 2, pp 419–435. doi:10.1007/978-94-007-0326-1_32

Gonzalez, W. D., Joselyn, J. A., Kamide, Y., Kroehl, H.W., Rostoker, G., Tsurutani, B. T. & Vasyliunas, V. (1994). What is a geomagnetic storm. *Journal of Geophysical Research*. 99, pp. 5771–5792.

Gopalswamy, N. (2009). Halo coronal mass ejections and geomagnetic storms. *Earth, Planets and Space*, 61, 5, pp 595–597. doi:10.1186/bf03352930

Gopalswamy, N., Yashiro, S., Akiyama, S., Mäkelä, P., Xie, H., Kaiser, M. L. & Bougeret, J. L. (2008). Coronal mass ejections, type II radio bursts, and solar energetic particle events in the SOHO era. *Annales Geophysicae*, 26, 10, pp. 3033-3047

Heelis, R. A. (2004). Electrodynamics in the low and middle latitude ionosphere: a tutorial. *Journal of Atmospheric and Solar-Terrestrial Physics*, 66, 10, pp 825–838. doi:10.1016/j.jastp.2004.01.034

Hughes, W. J. (1995), *The magnetopause, magnetotail and magnetic reconnection, in Introduction to Space Physics*, edited by M. G. Kivelson and C. T. Russell, Cambridge Univ. Press, Cambridge, UK.

Hunsucker, R. D.& Hargreaves, J. K., (2003), *The high-Latitude Ionosphere and Its Effects on Radio Propagation*. Cambridge University Press, New York.

Maruyama, N., Richmond, A. D., Fuller-Rowell, T. J., Codrescu, M. V., Sazykin, S., Toffoletto, F. R., et al. (2005)., Interactions between direct penetration and disturbance dynamo electric fields in the storm-time equatorial ionosphere. *Geophysical Research Letters*, 32, L17105. doi:10.1029/*2005GL023763*, *2005*.

Chakraborty, M., Kumar, S., Kumar D, B & Guha, A. (2015), Effects of geomagnetic storm on low latitude ionospheric total electron content: A case study from Indian sector. *Journal of Earth System Science*, DOI: 10.1007/s12040-015-0588-3

Nava, B., Rodríguez-Zuluaga, J., Alazo-Cuartas, K., Kashcheyev, A., Migoya-Orué, Y., Radicella, S. M., ... & Fleury, R. (2016). Middle-and low-latitude ionosphere response to 2015 St. Patrick's Day geomagnetic storm. *Journal of Geophysical Research: Space Physics*, 121, 4, 3421-3438.

Okpala, K. C., Ugwu, E. B., Attah, O. J., Obiegbuna, D., Anamezie, R. C. & Egbunu, F. (2020), Variation of vertical total electron content over West Africa during Geomagnetic storms. *Physical Science International Journal*, 24, 5, pp 52-63. Doi:10.9734/PSIJ/2020/v24i530193

Perreault, P., & Akasofu, S.-I. (1978), A study of geomagnetic storms. *Geophysical Journal International*, 54, 3, pp 547–573. doi:10.1111/j.1365-246x.1978.tb05494.x

Rishbeth, H. (1998). How the thermospheric circulation affects the ionospheric F2-layer. *Journal of Atmospheric and Solar-Terrestrial Physics*, 60, 14, pp 1385–1402. doi:10.1016/s1364-6826(98)00062-5

Sastri, J. H., Abdu, M. A. and Sobral, J. H. A., (1997), Response of equatorial ionosphere to episodes of asymmetric ring current activity, Annales Geophysicae, 15, pp 1316–1323, doi:10.1007/s00585-997-1316-3.

Seemala, G. K., & Valladares, C. E. (2011), Statistics of total electron content depletions observed over the South American continent for the year 2008. *Radio Science*, 46, 5, n/a–n/a. doi:10.1029/2011rs004722

Sharma, S. K., Singh, A. K., Panda, S. K., & Ahmed, S. S. (2020). The effect of geomagnetic storms on the total electron content over the low latitude Saudi Arab region: a focus on St. Patrick's Day storm. *Astrophysics and Space Science*, 365, pp. 2, pp 1-10.

Watari Shinichi (2017), Geomagnetic storms of solar cycle 24 and their solar sources, journal of *Earth, Planets and Space*, 69, 70. DOI:10.186/s40623-017-0653-z

Tsurutani, B. T., & Gonzalez, W. D. (1997), The Interplanetary causes of magnetic storms: A review. *Geophysical Monograph Series*, pp 77–89. doi:10.1029/gm098p0077

Watson, C., Jayachandran, P. T., & MacDougall, J. W. (2016), GPS TEC variations in the polar cap ionosphere: Solar wind and IMF dependence. *Journal of Geophysical Research: Space Physics*, 121, pp 9030– 9050, doi:10.1002/2016JA022937.

Yeh, H.-C., Foster, J. C., Rich, F.J., & Swider, W. (1991). Storm time electric field penetration observed at mid-latitude. *Journal of Geophysical Research*, 96, 4, pp 5707–5721. Doi:10.1029/90JA02751

Zhao, B., Wan, W., Tschu, K., Igarashi, K., Kikuchi, T., Nozaki, K., Watari, S., Li, G., Paxton, L. J., Liu, L., Ning, B., Liu, J.-Y., Su, S.-Y & Bulanon P.H., (2008), Ionospheric disturbances observed throughout southeast Asia of superstorm of 20–22 November 2003, *Journal of Geophysical Research*, 113 A00A04, doi: 10.1029/2008JA013054.

Sandhu, J.K., Rae, I.J., Freeman, M.P., Forsyth, C., Gkioulidou, M., Reeves, G.D., Spence, H.E., Jackman, C.M. & Lam, M.M. (2018), Energization of the ring current by Substorms. *Journal of Geophysical Research*, vol. 123, no. 10, pp. 8131 – 8146, 2018.

Cane, H.V., Richardson, I.G. & St. Cyr, O.C. (2000), Corona mas ejections, interplanetary ejecta and geomagnetic storms, *Geophysical research letters*, 27, 21, pp 3591-3594

Webb, D. F., Cliver, E.W., Crooker, N.U., St. Cyr, O.C. & Thompson, B.J. (2000), *Journal of Geophysical Research: Space Physics*, 105, A4, pp. 7491-7508.

Bounsanto, M.J. (1999), Ionospheric storms - a review, *Space Science Review*, 88, pp 563 – 601.

Forbes, M. (1989), Evidence for the equatorward penetration of electric fields, winds and compositional effects in the Asian/Pacific sector during the September 17-24, 1984 ETS interval, *Journal of Geophysical Research*, 9, 16, pp 999-1007,

Conflict of interest

The authors hereby declare that no conflicts of interest exist among the authors and that no funding was accessed for this study.